Published in final edited form as:

Pigment Cell Melanoma Res. 2016 January ; 29(1): 68–80. doi:10.1111/pcmr.12426.

Effective Intra-S Checkpoint Responses to UVC in Primary Human Melanocytes and Melanoma Cell Lines

Marila Cordeiro-Stone[1,2,3,4], **John J. McNulty**[1], **Christopher D. Sproul**[2], **Paul D. Chastain**[1], **Eugene Gibbs-Flournoy**[1], **Yingchun Zhou**[3], **Craig Carson**[5], **Shangbang Rao**[6], **David L. Mitchell**[7], **Dennis A. Simpson**[1], **Nancy E. Thomas**[3,4,5], **Joseph G. Ibrahim**[6], and **William K. Kaufmann**[1,2,3,4,*]

[1]Department of Pathology and Laboratory Medicine, University of North Carolina, Chapel Hill, NC

[2]Curriculum in Toxicology, University of North Carolina, Chapel Hill, NC

[3]Lineberger Comprehensive Cancer Center, University of North Carolina, Chapel Hill, NC

[4]Center for Environmental Health and Susceptibility, University of North Carolina, Chapel Hill, NC

[5]Department of Dermatology, University of North Carolina, Chapel Hill, NC

[6]Department of Biostatistics, University of North Carolina, Chapel Hill, NC

[7]Science Park – Research Division, The University of Texas MD Anderson Cancer Center, Smithville, TX

Summary

The objective of this study was to assess potential functional attenuation or inactivation of the intra-S checkpoint during melanoma development. Proliferating cultures of skin melanocytes, fibroblasts and melanoma cell lines were exposed to increasing fluences of UVC and intra-S checkpoint responses were quantified. Melanocytes displayed stereotypic intra-S checkpoint responses to UVC qualitatively and quantitatively equivalent to those previously demonstrated in skin fibroblasts. In comparison to fibroblasts, primary melanocytes displayed reduced UVC-induced inhibition of DNA strand growth and enhanced degradation of p21Waf1 after UVC, suggestive of enhanced bypass of UVC-induced DNA photoproducts. All nine melanoma cell lines examined, including those with activating mutations in *BRAF* or and *NRAS* oncogenes, also displayed proficiency in activation of the intra-S checkpoint in response to UVC irradiation. The results indicate that bypass of oncogene-induced senescence during melanoma development was not associated with inactivation of the intra-S checkpoint response to UVC-induced DNA replication stress.

Keywords

Human; melanocyte; melanoma; DNA replication; ultraviolet radiation; replicon initiation; intra-S checkpoint

*Corresponding author: Lineberger Cancer Center, 450 West Drive, University of North Carolina at Chapel Hill, Chapel Hill, NC 27599-7295; Phone: (919) 966-8209; wkarlk@med.unc.edu.

INTRODUCTION

Intra-S checkpoint responses are thought to contribute to genetic stability by delaying initiation of DNA replication at chromatin domains not yet replicated, decreasing fork displacement rates, and protecting stalled replication forks from breakage (Kaufmann, 2010). In cooperation with DNA repair pathways, these responses reduce the probability of replicating damaged DNA, which generates gene mutations and chromosomal aberrations (Kaufmann and Wilson, 1994; Konze-Thomas et al., 1982). It follows from these premises that attenuation or inactivation of the intra-S checkpoint would favor the accumulation of mutations induced by DNA damaging events, such as sunlight exposure, thus enhancing the risk for skin carcinogenesis. These considerations prompted the examination of the intra-S checkpoint in UVC-irradiated cultured cell lines to determine if defects in this signaling pathway might be common in melanoma. This study required the characterization of intra-S checkpoint responses in normal human melanocytes, the target cell type for melanomagenesis.

One of the major risk factors in the development of malignant melanoma is sunlight exposure (Gilchrest et al., 1999; Thomas et al., 2007), which produces two major types of DNA photolesions, cyclobutane pyrimidine dimers (CPDs) and 6–4 pyrimidine/pyrimidone photoproducts (6-4PP), as well as oxidative DNA base damage such as 8-oxo-deoxyguanine (8-oxo-dG). Nucleotide excision repair (NER) is the main line of defense against the genotoxicity of UV-induced DNA photolesions (Sancar et al., 2004). Cells that are not in S at the time of irradiation have more time to remove these lesions before engaging in DNA replication (Konze-Thomas et al., 1982) and the time for repair before replication is extended by the activation of cell cycle checkpoints (Kaufmann and Wilson, 1994). In addition to NER, cells entering the S phase with UV-induced DNA photolesions also rely on DNA damage tolerance pathways, such as translesion synthesis (TLS) and recombinational post-replication repair (PRR) to complete DNA replication and sustain viability (Kaufmann, 2010). Stalled forks that collapse into DNA double strand breaks (DSB) are repaired by homologous recombination and non-homologous end-joining (Kaufmann, 2010). S phase cells respond to UV-induced DNA damage by activating an ATR- and Chk1-dependent intra-S checkpoint (Heffernan et al., 2002), which remarkably does not appear to protect against UVC-induced *HPRT* mutations (Sproul et al., 2013).

Human cells express two intra-S checkpoint signaling pathways that have different DNA damage sensors and downstream signaling pathways (Ciccia and Elledge, 2010). The intra-S checkpoint response to ionizing radiation (IR)-induced DNA DSB is activated by recruitment and activation of ATM by the Mre11-Rad50-Nbs1 (MRN) complex. ATM phosphorylates Chk1 and Chk2, which phosphorylate other substrates such as Cdc25A to inhibit replicon initiation and DNA chain elongation in active replicons. The intra-S checkpoint response to UVC does not require ATM nor the MRN complex (Heffernan et al., 2002), but rather responds to the stalling of replication forks at UV-induced template damage with recruitment of ATR/ATRIP to RPA-coated single stranded DNA (Zou and Elledge, 2003). Rad17-dependent recruitment of the 9-1-1 complex further recruits the ATR cofactor TopBP1. ATR phosphorylates Chk1 and other substrates to stabilize stalled forks, inhibit replicon initiation and slow DNA chain elongation in active replicons. The biological

importance of the ATR/Chk1 signaling pathway is exemplified by its essential function in development; ATR- and Chk1-null mouse embryos are inviable and die in gestation (Brown and Baltimore, 2000; Liu et al., 2000). Both the ATM- and ATR-generated intra-S checkpoint signaling pathways may converge to evict Cdc45 from the replicative helicase complex on chromatin (Falck et al., 2002; Liu et al., 2006).

TLS across UV-induced CPDs relies upon Rad6/Rad18-mediated ubiquitylation of PCNA to switch replicative DNA polymerases with DNA pol eta (Durando et al., 2013). The p53-inducible, cyclin-dependent kinase inhibitor p21Waf1 also interacts with PCNA and may influence TLS. Remarkably, while p21Waf1 is induced by p53 4–24 h after UV-induced DNA damage (Gaddameedhi et al., 2010), ubiquitin-mediated proteolysis of p21Waf1 can reduce its abundance 1–3 h after UV treatment (Nishitani et al., 2008). Proteolysis of p21Waf1 was found to enhance pol eta interaction with PCNA, but not PCNA ubiquitylation after high fluences of UV (Mansilla et al., 2013; Soria et al., 2008).

Defects in NER and TLS sensitize humans to skin cancers, including melanoma, as evidenced by their higher incidence, and development at a much younger age, in patients with the genetic disease xeroderma pigmentosum (Kraemer et al., 1994). DNA damage checkpoint defects are common in many different types of cancer, especially for checkpoints operating in the G_1 and G_2 phases of the cell cycle (Carson et al., 2012; Kastan and Bartek, 2004; Omolo et al., 2013). It is thought that checkpoint defects destabilize the genome, enhancing the accumulation of gene mutations that drive carcinogenesis (Kaufmann and Kaufman, 1993; Negrini et al., 2010). However, it is not known if inactivation of the intra-S checkpoint is a common event in cancer pathogenesis. ATM is a well-established tumor suppressor (Reddy et al., 2010) and inactivation of ATM is seen in several lymphoid malignancies (Stankovic et al., 2002). Heterozygotes with reduced expression of ATR and Chk1 display accelerated malignant progression (Gilad et al., 2010; Lam et al., 2004). Erythroblast transformation-specific (ETS) family of transcription factors can repress expression of Chk1 and might play a role in prostate cancer (Lunardi et al., 2015). If the intra-S checkpoint were a major component of the arsenal for protection of the human genome, its inactivation might be expected in a fraction of human cancers, including melanomas. Alternatively, replication of the cancer cell genome might be so essential for the maintenance of the malignant state that cancer cells retain an intact intra-S checkpoint. This study indicates that defects in the UVC-induced, intra-S checkpoint are uncommon among melanoma cell lines consistent with its essential functions.

RESULTS

Normal human melanocytes are proficient in the intra-S checkpoint responses to UVC

DNA damage responses in S phase cells include the active inhibition of replicon initiation and the active and passive inhibition of DNA strand growth in operating replicons (Unsal-Kacmaz et al., 2007). The active intra-S checkpoint responses can be detected by various methods with different resolution powers. For instance, the overall rate of DNA synthesis within the first 30–60 min after exposure to low fluences of UVC (1–2 J/m^2) is significantly reduced in human cells with an operational intra-S checkpoint (Heffernan et al., 2002; Unsal-Kacmaz et al., 2005). Using this parameter, three independently derived strains of

normal human melanocytes were compared to three different lines of diploid human fibroblasts immortalized by ectopic expression of the catalytic subunit of human telomerase (hTERT)(Heffernan et al., 2002). The melanocytes as a group displayed results similar to the fibroblasts (Supplementary Figure S1), suggesting that melanocytes were capable of activating the intra-S checkpoint, as previously demonstrated for fibroblasts (Heffernan et al., 2002).

Velocity sedimentation of DNA through alkaline sucrose gradients discloses the steady-state distribution of sizes of single stranded nascent DNA; UVC-induced alterations in this distribution can be used to deduce both active and passive effects of DNA damage on DNA replication (Painter and Young, 1980; Wang et al., 2004). A selective inhibition in the labeling of low molecular weight nascent DNA (<60 kb, sub-replicon size, origin-proximal molecules) in cultures exposed to a low fluence of UVC (1 J/m^2 in Figure 1) is indicative of the inhibition of replicon initiation (Kaufmann and Cleaver, 1981; Kaufmann et al., 1980). By comparison, a high fluence (10 J/m^2 in Figure 1) caused a reduction in labeled high molecular weight DNA, which coincided with the appearance of a new peak of very small labeled DNA molecules. This pattern reflects the passive blockage of DNA polymerases at template lesions and the accumulation of daughter strand gaps. Based on these pattern interpretations, the results in Figure 1 demonstrate that two of three melanocyte strains activated the intra-S checkpoint in response to exposure to 1 J/m^2 UVC. Such a response was robust in NHM16 (Figure 1A) and NHM18 (Figure 1B), but it seemed to be absent in NHM28 (Figure 1C). The results shown in Figure 2A, however, demonstrate that such an interpretation would be premature; a pattern of response consistent with the active inhibition of replicon initiation was observed in NHM28 upon exposure to 2.5 (Supplementary Figure S2) or 3 J/m^2 UVC (Figure 2A). The attenuated responses in NHM28 appear to be related to a higher level of pigmentation (see below).

The UVC fluence-dependent inhibition of DNA strand growth was quantified by measuring the average reduction in radiolabeled precursor incorporation into high molecular weight DNA intermediates (Figure 2A). All three melanocyte lines were more resistant to the inhibition of DNA strand growth by UVC than normal fibroblasts (Figure 2B) and statistical comparison of NHM16/NHM18 and NHF revealed a significant difference between the slopes ($p=0.0023$). NHM28 showed an apparent shoulder in the fluence-dependent inhibition of DNA strand growth (consistent with results shown above), but a similar slope to that observed for NHM16 and NHM18. For comparison, Figure 2B also shows how this assay differentiates NHF from xeroderma pigmentosum variant (XP-V) fibroblasts ($p<0.0001$), which are defective in DNA pol eta-dependent TLS of CPD (King et al., 2005).

Fiber spreading and immunostaining permit visualization of replication tracks in individual DNA molecules and provide independent confirmation of inhibition of replicon initiation and DNA chain elongation (Chastain et al., 2006; Unsal-Kacmaz et al., 2007). Using this method, immortalized human melanocytes (NHM4-hTERT) exposed to low fluences of UVC (1–2.5 J/m^2) displayed a reduction of 25–40% in the proportion of green-only replication tracks, i.e. those into which only the DNA precursor added to the cultures after irradiation was incorporated, thus reflecting the inhibition of replicon initiation (Figure 3A). Such inhibition is maintained at higher fluences of UVC (5–10 J/m^2), an effect that could

not be evaluated by using the methods described above. Units of DNA replication that were activated before the UVC treatment and continued to replicate during the subsequent pulse generated replication tracks containing both IdU (pre-UVC label and stained red) and CldU (post-UVC label and stained green). By measuring the length of the green regions in the red-green tracks, it was possible to determine the average inhibition of DNA chain elongation (Figure 3B). The sharp reduction in track length observed after 1 J/m^2, relative to the sham-irradiated control, is most consistent with an active checkpoint response that slows the rate of progression of DNA replication forks. As lesion density was increased at higher UVC fluences, there was a more gradual decrease in track length, reflecting the contribution of passive blockage of replication forks at template lesions.

Melanin and the molecular dosimetry of UVC-induced CPDs in melanocytes

The possibility of attenuation of DNA lesion densities induced by the incident UVC fluences, due to the variable melanin content in melanocyte strains and melanoma cell lines (Swope et al., 2014), required measurements of a marker of molecular dose to validate comparisons of DNA damage responses (e.g. Figures 1&2). CPDs are the most abundant lesions induced in DNA by UVC; they were measured by quantitative immunoblotting, using an internal standard curve constructed with calf thymus DNA for which the CPD density had been previously determined by radio-immunoassay (Sproul et al., 2014). Results illustrated in Figure 4 show that in NHM28 the CPD/Mb content was lower than in fibroblasts and NHM16 melanocytes at each of the UVC fluences used to irradiate the cultures. These results were correlated with melanin content. The concentration of melanin in NHM28 melanocytes was 39 μg/10^6 cells while the melanin concentration in NHM16 melanocytes was 15 μg/10^6 cells. Fibroblasts had no detectable melanin. In the lightly pigmented NHM16, the CPD densities were indistinguishable from those detected in the non-pigmented fibroblasts. A second radio-immunoassay also showed similar UVC-induced CPD densities in lightly pigmented primary NHM4 cultures (6 μg melanin/10^6 cells) when compared directly with fibroblasts (results not shown).

Protein markers of DNA damage responses

Whole cell extracts from fibroblasts and melanocytes were probed for several molecular markers of the DNA damage response 45 min after treatment with low fluences of UVC (Figure 5). Fibroblasts and melanocytes displayed qualitatively and quantitatively similar responses to UVC with induction of P-ATM, P-Chk1, P-Chk2 and P-H2AX. Although melanocytes and fibroblasts expressed similar levels of ATM when equal amounts of protein were loaded onto gels, melanocytes displayed a higher basal level of P-ATM. The fold induction of P-ATM by UVC was, however, similar in fibroblasts and melanocytes. The NHM16 and NHM18 melanocyte strains displayed a substantial decrease in abundance of p21Waf1 after UVC with 80% reduction after 4 J/m^2. This UVC-induced reduction of p21Waf1 was less pronounced in the fibroblasts. The NHM28 melanocyte strain displayed similar levels of activation of checkpoint kinases as seen in the other melanocytes but only a 20% decrease in p21Waf1 after 4 J/m^2 (Supplementary Figure S3), consistent with less UV-induced DNA damage.

Melanoma cells retain the intra-S checkpoint

Having established that normal human melanocytes displayed an effective intra-S checkpoint response to UVC, we then inspected melanoma cell lines by velocity sedimentation analysis. Nine cell lines were selected among those expressing oncogenic B-Raf or N-Ras, or the wild-type alleles for these two signaling proteins (Supplementary Table S1). The intent was to determine whether potential deficiencies in intra-S checkpoint responses to UVC correlated with either of these two mutations that are common in melanomas (Daniotti et al., 2004; Thomas et al., 2007). The results illustrated in Figure 6 show that all nine melanoma cell lines activated the intra-S checkpoint response of inhibition of replicon initiation after the low 1 J/m^2 fluence of UVC. Note, however, that the degree of inhibition of DNA strand growth at 10 J/m^2 UVC, as well as the relative accumulation of abnormally small nascent DNA, varied among the melanomas (see Supplementary Figure S4 for the results with intermediate fluences).

The nine melanoma cell lines used in this study displayed low to no pigmentation; accordingly, four of them were tested directly and displayed no variation in UVC-induced CPD density relative to human fibroblasts (Supplementary Figure S5). Therefore, their responses to UVC, reported on the basis of the incident UVC fluences, can be compared to those observed in the NHM16 and NHM18 melanocyte strains.

All nine melanoma cell lines showed induction of phosphorylation of Chk1 kinase (as a reporter of ATR activation) (Figure 7), as was expected based on their proficiency in the intra-S checkpoint response documented above. Note that in RPMI 8322 there was a strong signal for phospho-Chk1 even at the lowest UVC fluence.

Post-replication repair capacity in melanocytes and melanoma cell lines

Post-replication repair (PRR) denotes a collection of pathways that remove DNA replication mistakes (mismatch repair) and promotes the completion of genome replication despite the presence of lesions on DNA templates (TLS and daughter strand gap repair). Differences in PRR capacity are reflected in the slopes of the UVC fluence-dependent inhibition of DNA strand growth (Table 1), as illustrated in Figure 2B when comparing melanocytes and fibroblasts. Similar analysis for melanoma cell lines (Figure 8) revealed a range of UVC fluence-dependent inhibition of DNA strand growth. There was modest variation among most of the melanoma cell lines with generally less than 2-fold variation in slopes (Table 1). Some melanoma lines were less sensitive than the melanocytes (SKMel-187, SKMel-23) and some were more sensitive (SKMel-103, SKMel-147 and A2058). Noteworthy was the enhanced sensitivity of RPMI 8322 by comparison to either normal melanocytes or the other melanoma cell lines ($p<0.0001$). The strong inhibition of [^{3}H]thymidine in high molecular weight DNA in RPMI 8322 was also associated with an accumulation of abnormally small nascent DNA that peaked above the sham-treated control profile (Figure 6 and Supplementary Figure S4), resembling the behavior of TLS-defective XP-V fibroblasts (Kaufmann and Cleaver, 1981). This observation prompted the analysis of DNA polymerase eta in RPMI 8322.

Western immunoblot analysis of unfractionated cell lysates demonstrated expression of pol eta in RPMI 8322 at a level similar to that seen in NHM16 melanocytes but lower than seen in four other melanoma cell lines (results not shown). To quantify pol eta and its response to UVC, chromatin was isolated 45 min after sham treatment or irradiation with 10 J/m^2 UVC and equal masses of protein were evaluated by western immunoblotting (Figure 9). RPMI 8322 showed a lower abundance of DNA pol eta on chromatin than the A375 melanoma cell line but similar abundance to that observed in NHM16 melanocytes. Pol eta association with chromatin did not change with UVC treatment. Expression of PCNA on chromatin was stimulated substantially by UVC, most noticeably in the XP-V and NHM16 samples. The NHF1-hTERT fibroblasts displayed a similar induction of PCNA binding to chromatin after UVC (not shown). The melanoma lines displayed a high basal level of expression of PCNA on chromatin with little additional binding after UVC. Contamination of the chromatin fraction with the cytoplasmic protein α-tubulin was highest in the XP-V fibroblast line but equivalent among the melanocyte and melanoma lines. Normalized to PCNA expression on chromatin, the level of pol eta in RPMI 8322 was substantially less than seen in A375.

Microarray analysis of mRNA expression (Carson et al., 2012) also revealed reduced expression of pol eta in RPMI 8322 in comparison to melanocytes and other melanoma cell lines, which was validated by quantitative PCR (Supplementary Figure S6). Sequence analysis using exon-capture and duplex consensus sequencing (Schmitt et al., 2012) did not detect any mutation in pol eta that could explain the observed responses of RPMI 8322 (results not shown). Nonetheless, RPMI 8322 displayed enhanced UVC cytotoxicity in the presence of caffeine (Supplementary Figure S7), which is a phenomenon also observed in XPV cells with mutant, non-functional DNA pol eta (Kaufmann et al., 2003; Yamada et al., 2000).

DISCUSSION

To our knowledge, this study reports the first demonstrations of UVC-induced intra-S checkpoint function and TLS in primary cultures of human melanocytes. Melanocytes have been shown to respond to UVC as well as UVB/UVA with activation of ATM, ATR and Chk1, induction of p53 and p21Waf1, and arrest in G1 and G2 (Gaddameedhi et al., 2010; Kowalczuk et al., 2006; Medrano et al., 1995 ; Swope et al., 2014). The intra-S checkpoint response to UVC was detected in normal human melanocytes at levels and with characteristics similar to those previously reported in normal human fibroblasts (Cistulli and Kaufmann, 1998; Cordeiro-Stone et al., 2002; Heffernan et al., 2002; Heffernan et al., 2007). Low fluences of UVC activated Chk1 and significantly inhibited replicon initiation and DNA chain elongation in both cell types. Remarkably, even after consideration of potential differences in UVC-induced DNA photolesion density, melanocytes displayed reduced sensitivity to UVC-induced inhibition of DNA chain elongation in comparison to fibroblasts. As melanocytes displayed robust activation of Chk1, this reduced inhibition of DNA replication did not appear to be due to attenuation of checkpoint signaling that inhibits DNA chain elongation (Unsal-Kacmaz et al., 2007). Fiber spreading with immuno-staining demonstrated a 25% inhibition of DNA chain elongation at the low 1 J/m^2 fluence of UVC consistent with active inhibition by the intra-S checkpoint. Irradiated melanocytes also displayed greater reduction in p21Waf1 abundance than fibroblasts. UVC-induced

degradation of p21Waf1 is mediated by ubiquitylation (Abbas et al., 2008) and may facilitate TLS by enhancing the interaction of DNA pol eta with PCNA (Mansilla et al., 2013). These results suggest that melanocytes express significantly better TLS/PRR than fibroblasts. As skin melanocytes commonly receive damage by solar UVB they can be expected to display effective protections against UV-induced genotoxicity. Melanocytes expressed a p53-independent G2 checkpoint response to IR-induced DNA DSB equivalent to that seen in fibroblasts, but an attenuated p53-dependent G1 checkpoint response to DSB (about half of that seen in fibroblasts) (Carson et al., 2012; Omolo et al., 2013). Thus, human skin cells display highly stereotypic responses to DNA damage, but cell-type-specific variations in the intensities of response.

Analyses of DNA damage responses in cancer and its precursors suggest that DNA replication stress may be an early event contributing to genomic instability (Negrini et al., 2010). Ectopic expression of oncogenic B-Raf or N-Ras induced P-H2AX in normal human melanocytes (Haferkamp et al., 2009; Suram et al., 2012) and oncogenic N-Ras induced a p53- and RB-dependent growth arrest in such cells (Haferkamp et al., 2009). DNA damage checkpoint responses to oncogene-induced replication stress appear to represent barriers to cancer development and the inactivation or attenuation of p53-dependent G1 checkpoint function in melanoma cell lines (Carson et al., 2012) may provide one mechanism for barrier bypass. B-Raf-induced senescence in human melanocytes was not reversed by inactivation of p53 (Kuilman et al., 2010), but was reversed by deletion of PTEN (Vredeveld et al., 2012). A potential cooperation between oncogenic *BRAF* and deletion of *PTEN* is evident from analysis of melanomas and melanoma cell lines (Daniotti et al., 2004; Kaufmann et al., 2014). Melanoma cell lines with activating mutations in *BRAF* or *NRAS* and lines with wildtype oncogenes displayed effective intra-S checkpoint responses to UVC. The central signaling molecules in the intra-S checkpoint response to UVC (ATR and Chk1) are essential for embryonic development (Brown and Baltimore, 2000; Liu et al., 2000); thus, it may be that melanoma cell lines retain effective ATR and Chk1 signaling pathways because they cannot live without them. This conclusion is supported by the demonstration that conditional inactivation of Chk1 in murine melanocytes blocked coat pigmentation and melanocyte presence in hair follicles (Smith et al., 2013). The essential nature of ATR and Chk1 favors the application of ATR and Chk1 inhibitors for melanoma therapy. We found that two-thirds of melanoma cell lines displayed a defective p53-dependent G1 checkpoint response to IR (Carson et al., 2012) and another study concluded that p53-signaling was defective in melanoma (Yu et al., 2009). As Chk1 inhibitors appear to be especially effective in cancer lines with defective p53 function (Origanti et al., 2013), a majority of melanomas may be effectively targeted by Chk1 inhibition.

The RPMI 8322 melanoma line represents an example of a cancer cell line with severe defects in many elements of DNA damage response. It displays high expression of mutant p53 protein (Gaddameedhi et al., 2010), no expression of p21Waf1, even after exposure to UVC (Gaddameedhi et al., 2010) or ionizing radiation (Kaufmann et al., 2008), high basal expression of P-Chk2 and P-H2AX (Nikolaishvilli-Feinberg et al., 2014), severely reduced excision repair of CPDs (Gaddameedhi et al., 2010), hypersensitivity to UVC-induced cytotoxicity in the absence (Gaddameedhi et al., 2010) and presence of caffeine

(Supplementary Figure S7), and hypersensitivity to UVC-induced inhibition of DNA strand growth (Figure 9) with overproduction of abnormally small nascent DNA (Figure 6 and Supplementary Figure S4). Although mutational inactivation of p53 was associated with reduced NER of CPDs in melanoma cell lines (Gaddameedhi et al., 2010), other p53-mutant melanoma lines displayed much greater repair of CPDs than RPMI 8322, suggesting a defect in NER beyond that associated with inactivation of p53. As RPMI 8322 did not express p21Waf1, the hypersensitivity to inhibition of strand growth could not be attributed to retention of p21Waf1 on PCNA to block pol eta-dependent TLS (Mansilla et al., 2013). Expression of pol eta mRNA and protein was very low in RPMI 8322, well below that measured in melanoma cell lines with apparently effective TLS and PRR (Figure 9, Supplementary Figure S6). Given the coincidence of reduced pol eta expression and hypersensitivities to UVC-induced inhibitions of strand growth, production of small nascent DNA, and caffeine-enhanced cytotoxicity, all attributes of XPV cells, we conclude that RPMI 8322 has an XPV-like defect in DNA damage response. As no exon mutation in *POLH* was detected, it would appear that some defect that affects synthesis and/or stability of the mRNA or the protein might be responsible for the low abundance of DNA pol eta and UVC hypersensitivity in RPMI 8322. Alternatively, reduced recruitment and/or access of DNA pol eta to replication sites blocked at a CPD on the template strand could possibly explain the XPV-like phenotype of RPMI 8322.

METHODS

Cell lines

Human foreskin fibroblast lines were grown as previously described (Cordeiro-Stone et al., 2002; Heffernan et al., 2002). Melanocytes were derived from newborn human foreskin and cultured in medium 254 containing human melanocyte growth supplement 2 (HMGS-2; Invitrogen™, Life Technologies™) (Carson et al., 2012), with the exception of the NHM28 strain, which was cultured in Dermalife® M medium (Lifeline Cell Technology®). Secondary cultures of NHM4 melanocytes were transduced with the catalytic subunit of human telomerase, as previously described (Heffernan et al., 2002). Melanoma cell lines were cultured in Dulbecco's Modified Eagle Medium (DMEM, Gibco®, Life Technologies™) or in RPMI-1640 medium (Gibco®) supplemented with 10% fetal calf serum and 1 mM glutamine (Carson et al., 2012). Memorial Sloan Kettering Cancer Center provided the SK-Mel cell lines. All cultures were incubated at 37°C in an atmosphere of 95% ambient air and 5% CO_2. Stock cultures were maintained in antibiotic-free medium and confirmed to lack mycoplasma contamination as previously described (Carson et al., 2012). Melanin content of melanocyte and melanoma cell cultures was determined as described in Watts *et al*. (Watts et al., 1981).

UV Irradiation

Medium was removed from exponentially growing cultures and reserved. Cells were washed once with pre-warmed phosphate-buffered saline (PBS); after removing the PBS, the uncovered plates were placed under a germicidal lamp emitting primarily 254 nm UVC. The incident UVC fluence rate was about 0.5 J/m^2/sec and it was measured periodically with a UVX-25 sensor and a digital radiometer (UVP, Inc., Upland, CA) to ensure reproducibility.

After irradiation (or sham-treatment) reserved medium was replaced and the cultures returned to the incubator.

Determination of cyclobutane pyrimidine dimer (CPD) density

The methodologies for DNA immunoblotting with anti-CPD antibodies, the use of standard curves and the radio-immuno assays (RIA) performed in David Mitchell's laboratory were described previously (Sproul et al., 2014).

Quantitative analysis of DNA replication

The velocity sedimentation method, for quantifying UVC-induced alterations in the incorporation of [^{3}H]thymidine into DNA and the distribution of sizes of nascent DNA molecules, was done as previously described in detail (Heffernan et al., 2002; Kaufmann et al., 1980). For analysis of radioresistant DNA synthesis, cell cultures were incubated with [^{14}C]thymidine, exposed to increasing fluences of UVC and 30 min later pulse-labeled for 15 min with [^{3}H]thymidine; the specific activity of radiolabeled precursor incorporation (^{3}H/^{14}C) was measured by scintillation spectrometry after acid-precipitation of macromolecules from cell lysates (Chastain et al., 2006; Heffernan et al., 2002). The methods used to label NHM4-hTERT melanocytes with thymidine analogs IdU and CldU, to spread the DNA fibers, and to immunostain them were as published (Chastain et al., 2015; Chastain et al., 2006), except that the lengths of the pulses before (with IdU) and after (with CldU) UVC irradiation were 15 and 30 min, respectively.

Protein Immunoblotting

Immunoblot analysis of protein expression was done as previously described (Bower et al., 2010; Heffernan et al., 2007). To quantify the ratios of phosphorylated to total protein, the membranes were stripped after probing for the phosphorylated form, and re-probed for the total protein. Protein content in chromatin was determined as described (Liu et al., 2006). Sources of antibodies used in this study were: Chk1 (Santa Cruz Biotechnology), Phospho-ser345-Chk1 (Cell Signaling), Chk2 (BD Biosciences), Phospho-thr68-Chk2 (Cell Signaling), DNA polymerase eta (Abcam), H2A.X (Millipore), P-ser139-H2A.X (Santa Cruz Biotechnology), ATM (Santa Cruz Biotechnology), P-ser-1981-ATM (Epitomics), β-Actin (Santa Cruz Biotechnology), α-tubulin (Cell Signaling) and PCNA (Santa Cruz Biotechnology). HRP-conjugated, secondary antibodies used were goat anti-rabbit IgG (Santa Cruz Biotechnology), donkey anti-rabbit IgG (GE Healthcare), bovine anti-goat IgG (Santa Cruz Biotechnology), and sheep anti-mouse IgG (GE Healthcare).

Statistical Analysis

Mean rates of DNA synthesis in UVC-treated melanocytes and fibroblasts were compared for statistically significant differences using a two-sided T test with unequal variances. The SAS/STAT9.2 biostatistics software package was used to compare the UVC-fluence-dependent inhibitions of DNA strand growth in fibroblasts, melanocytes and melanoma cell lines. The variable for the main analysis was the log10 transformation of the percent inhibition of DNA strand growth with increasing UVC fluences, relative to the non-irradiated (sham-treated) control. To determine if the slopes of the inhibition of DNA strand

growth differed for different melanoma cell lines and in comparison to normal melanocytes a linear model was used with PROC GLM, which tested the slope differences using CONTRAST statements in GLM.

Supplementary Material

Refer to Web version on PubMed Central for supplementary material.

Acknowledgments

This study was supported by US Public Health Service research grants RO1 ES015856 (MCS) and P01 ES014635 (WKK) and by the training grants T32 ES007017 (Environmental Pathology) for traineeship awards to John J. McNulty and T32 ES007126 (Curriculum in Toxicology) for traineeship awards to Christopher D. Sproul. We acknowledge the contributions of the UNC-CH Lineberger Comprehensive Cancer Center (P30-CA16086) and UNC-CH Center for Environmental Health and Susceptibility (P30 ES10126). We are very thankful for the help received from Drs. Bruna P. Brylawski and Michael Durando and Mr. David C. Gibbs during the development of these studies. We thank Drs. Jayne Boyer and Leena Nylander-French for providing the NHM28 primary melanocyte strain.

References

Abbas T, Sivaprasad U, Terai K, Amador V, Pagano M, Dutta A. PCNA-dependent regulation of p21 ubiquitylation and degradation via the CRL4Cdt2 ubiquitin ligase complex. Genes & development. 2008; 22:2496–2506. [PubMed: 18794347]

Bower JJ, Zhou Y, Zhou T, Simpson DA, Arlander SJ, Paules RS, Cordeiro-Stone M, Kaufmann WK. Revised genetic requirements for the decatenation G2 checkpoint: the role of ATM. Cell cycle. 2010; 9:1617–1628. [PubMed: 20372057]

Brown EJ, Baltimore D. ATR disruption leads to chromosomal fragmentation and early embryonic lethality. Genes & development. 2000; 14:397–402. [PubMed: 10691732]

Carson C, Omolo B, Chu H, Zhou Y, Sambade MJ, Peters EC, Tompkins P, Simpson DA, Thomas NE, Fan C, et al. A prognostic signature of defective p53-dependent G1 checkpoint function in melanoma cell lines. Pigment cell & melanoma research. 2012; 25:514–526. [PubMed: 22540896]

Chastain PD, Brylawski BP 2nd, Zhou YC, Rao S, Chu H, Ibrahim JG, Kaufmann WK, Cordeiro-Stone M. DNA damage checkpoint responses in the S phase of synchronized diploid human fibroblasts. Photochemistry and photobiology. 2015; 91:109–116. [PubMed: 25316620]

Chastain PD 2nd, Heffernan TP, Nevis KR, Lin L, Kaufmann WK, Kaufman DG, Cordeiro-Stone M. Checkpoint regulation of replication dynamics in UV-irradiated human cells. Cell cycle. 2006; 5:2160–2167. [PubMed: 16969085]

Ciccia A, Elledge SJ. The DNA damage response: making it safe to play with knives. Molecular cell. 2010; 40:179–204. [PubMed: 20965415]

Cistulli CA, Kaufmann WK. p53-dependent signaling sustains DNA replication and enhances clonogenic survival in 254 nm ultraviolet-irradiated human fibroblasts. Cancer research. 1998; 58:1993–2002. [PubMed: 9581844]

Cordeiro-Stone M, Frank A, Bryant M, Oguejiofor I, Hatch SB, Mcdaniel LD, Kaufmann WK. DNA damage responses protect xeroderma pigmentosum variant from UVC-induced clastogenesis. Carcinogenesis. 2002; 23:959–965. [PubMed: 12082017]

Daniotti M, Oggionni M, Ranzani T, Vallacchi V, Campi V, Di Stasi D, Torre GD, Perrone F, Luoni C, Suardi S, et al. BRAF alterations are associated with complex mutational profiles in malignant melanoma. Oncogene. 2004; 23:5968–5977. [PubMed: 15195137]

Durando M, Tateishi S, Vaziri C. A non-catalytic role of DNA polymerase eta in recruiting Rad18 and promoting PCNA monoubiquitination at stalled replication forks. Nucleic acids research. 2013; 41:3079–3093. [PubMed: 23345618]

Falck J, Petrini JH, Williams BR, Lukas J, Bartek J. The DNA damage-dependent intra-S phase checkpoint is regulated by parallel pathways. Nature genetics. 2002; 30:290–294. [PubMed: 11850621]

Gaddameedhi S, Kemp MG, Reardon JT, Shields JM, Smith-Roe SL, Kaufmann WK, Sancar A. Similar nucleotide excision repair capacity in melanocytes and melanoma cells. Cancer research. 2010; 70:4922–4930. [PubMed: 20501836]

Gilad O, Nabet BY, Ragland RL, Schoppy DW, Smith KD, Durham AC, Brown EJ. Combining ATR suppression with oncogenic Ras synergistically increases genomic instability, causing synthetic lethality or tumorigenesis in a dosage-dependent manner. Cancer research. 2010; 70:9693–9702. [PubMed: 21098704]

Gilchrest BA, Eller MS, Geller AC, Yaar M. The pathogenesis of melanoma induced by ultraviolet radiation. The New England journal of medicine. 1999; 340:1341–1348. [PubMed: 10219070]

Haferkamp S, Tran SL, Becker TM, Scurr LL, Kefford RF, Rizos H. The relative contributions of the p53 and pRb pathways in oncogene-induced melanocyte senescence. Aging. 2009; 1:542–556. [PubMed: 20157537]

Heffernan TP, Simpson DA, Frank AR, Heinloth AN, Paules RS, Cordeiro-Stone M, Kaufmann WK. An ATR- and Chk1-dependent S checkpoint inhibits replicon initiation following UVC-induced DNA damage. Molecular and cellular biology. 2002; 22:8552–8561. [PubMed: 12446774]

Heffernan TP, Unsal-Kacmaz K, Heinloth AN, Simpson DA, Paules RS, Sancar A, Cordeiro-Stone M, Kaufmann WK. Cdc7-Dbf4 and the human S checkpoint response to UVC. The Journal of biological chemistry. 2007; 282:9458–9468. [PubMed: 17276990]

Kastan MB, Bartek J. Cell-cycle checkpoints and cancer. Nature. 2004; 432:316–323. [PubMed: 15549093]

Kaufmann WK. The human intra-S checkpoint response to UVC-induced DNA damage. Carcinogenesis. 2010; 31:751–765. [PubMed: 19793801]

Kaufmann WK, Carson CC, Omolo B, Filgo AJ, Sambade MJ, Simpson DA, Shields JM, Ibrahim JG, Thomas NE. Mechanisms of chromosomal instability in melanoma. Environmental and molecular mutagenesis. 2014; 55:457–471. [PubMed: 24616037]

Kaufmann WK, Cleaver JE. Mechanisms of inhibition of DNA replication by ultraviolet light in normal human and xeroderma pigmentosum fibroblasts. Journal of molecular biology. 1981; 149:171–187. [PubMed: 7310880]

Kaufmann WK, Cleaver JE, Painter RB. Ultraviolet radiation inhibits replicon initiation in S phase human cells. Biochimica et biophysica acta. 1980; 608:191–195. [PubMed: 7388031]

Kaufmann WK, Heffernan TP, Beaulieu LM, Doherty S, Frank AR, Zhou Y, Bryant MF, Zhou T, Luche DD, Nikolaishvili-Feinberg N, et al. Caffeine and human DNA metabolism: the magic and the mystery. Mutation research. 2003; 532:85–102. [PubMed: 14643431]

Kaufmann WK, Kaufman DG. Cell cycle control, DNA repair and initiation of carcinogenesis. FASEB journal : official publication of the Federation of American Societies for Experimental Biology. 1993; 7:1188–1191. [PubMed: 8375618]

Kaufmann WK, Nevis KR, Qu P, Ibrahim JG, Zhou T, Zhou Y, Simpson DA, Helms-Deaton J, Cordeiro-Stone M, Moore DT, et al. Defective cell cycle checkpoint functions in melanoma are associated with altered patterns of gene expression. The Journal of investigative dermatology. 2008; 128:175–187. [PubMed: 17597816]

Kaufmann WK, Wilson SJ. G1 arrest and cell-cycle-dependent clastogenesis in UV-irradiated human fibroblasts. Mutation research. 1994; 314:67–76. [PubMed: 7504193]

King NM, Nikolaishvili-Feinberg N, Bryant MF, Luche DD, Heffernan TP, Simpson DA, Hanaoka F, Kaufmann WK, Cordeiro-Stone M. Overproduction of DNA polymerase eta does not raise the spontaneous mutation rate in diploid human fibroblasts. DNA repair. 2005; 4:714–724. [PubMed: 15886068]

Konze-Thomas B, Hazard RM, Maher VM, Mccormick JJ. Extent of excision repair before DNA synthesis determines the mutagenic but not the lethal effect of UV radiation. Mutation research. 1982; 94:421–434. [PubMed: 7110182]

Kowalczuk CI, Priestner MC, Pearson AJ, Saunders RD, Bouffler SD. Wavelength dependence of cellular responses in human melanocytes and melanoma cells following exposure to ultraviolet radiation. International journal of radiation biology. 2006; 82:781–792. [PubMed: 17148262]

Kraemer KH, Levy DD, Parris CN, Gozukara EM, Moriwaki S, Adelberg S, Seidman MM. Xeroderma pigmentosum and related disorders: examining the linkage between defective DNA repair and cancer. The Journal of investigative dermatology. 1994; 103:96S–101S. [PubMed: 7963692]

Kuilman T, Michaloglou C, Mooi WJ, Peeper DS. The essence of senescence. Genes & development. 2010; 24:2463–2479. [PubMed: 21078816]

Lam MH, Liu Q, Elledge SJ, Rosen JM. Chk1 is haploinsufficient for multiple functions critical to tumor suppression. Cancer cell. 2004; 6:45–59. [PubMed: 15261141]

Liu P, Barkley LR, Day T, Bi X, Slater DM, Alexandrow MG, Nasheuer HP, Vaziri C. The Chk1-mediated S-phase checkpoint targets initiation factor Cdc45 via a Cdc25A/Cdk2-independent mechanism. The Journal of biological chemistry. 2006; 281:30631–30644. [PubMed: 16912045]

Liu Q, Guntuku S, Cui XS, Matsuoka S, Cortez D, Tamai K, Luo G, Carattini-Rivera S, Demayo F, Bradley A, et al. Chk1 is an essential kinase that is regulated by Atr and required for the G(2)/M DNA damage checkpoint. Genes & development. 2000; 14:1448–1459. [PubMed: 10859164]

Lunardi A, Varmeh S, Chen M, Taulli R, Guarnerio J, Ala U, Seitzer N, Ishikawa T, Carver BS, Hobbs RM, et al. Suppression of CHK1 by ETS Family Members Promotes DNA Damage Response Bypass and Tumorigenesis. Cancer discovery. 2015; 5:550–563. [PubMed: 25653093]

Mansilla SF, Soria G, Vallerga MB, Habif M, Martinez-Lopez W, Prives C, Gottifredi V. UV-triggered p21 degradation facilitates damaged-DNA replication and preserves genomic stability. Nucleic acids research. 2013; 41:6942–6951. [PubMed: 23723248]

Medrano EE, Im S, Yang F, Abdel-Malek ZA. Ultraviolet B light induces G1 arrest in human melanocytes by prolonged inhibition of retinoblastoma protein phosphorylation associated with long-term expression of the p21Waf-1/SDI-1/Cip-1 protein. Cancer research. 1995; 55:4047–4052. [PubMed: 7664278]

Negrini S, Gorgoulis VG, Halazonetis TD. Genomic instability--an evolving hallmark of cancer. Nature reviews. Molecular cell biology. 2010; 11:220–228. [PubMed: 20177397]

Nikolaishvilli-Feinberg N, Cohen SM, Midkiff B, Zhou Y, Olorvida M, Ibrahim JG, Omolo B, Shields JM, Thomas NE, Groben PA, et al. Development of DNA damage response signaling biomarkers using automated, quantitative image analysis. The journal of histochemistry and cytochemistry : official journal of the Histochemistry Society. 2014; 62:185–196. [PubMed: 24309508]

Nishitani H, Shiomi Y, Iida H, Michishita M, Takami T, Tsurimoto T. CDK inhibitor p21 is degraded by a proliferating cell nuclear antigen-coupled Cul4-DDB1Cdt2 pathway during S phase and after UV irradiation. The Journal of biological chemistry. 2008; 283:29045–29052. [PubMed: 18703516]

Omolo B, Carson C, Chu H, Zhou Y, Simpson DA, Hesse JE, Paules RS, Nyhan KC, Ibrahim JG, Kaufmann WK. A prognostic signature of G(2) checkpoint function in melanoma cell lines. Cell cycle. 2013; 12:1071–1082. [PubMed: 23454897]

Origanti S, Cai SR, Munir AZ, White LS, Piwnica-Worms H. Synthetic lethality of Chk1 inhibition combined with p53 and/or p21 loss during a DNA damage response in normal and tumor cells. Oncogene. 2013; 32:577–588. [PubMed: 22430210]

Painter RB, Young BR. Radiosensitivity in ataxia-telangiectasia: a new explanation. Proceedings of the National Academy of Sciences of the United States of America. 1980; 77:7315–7317. [PubMed: 6938978]

Reddy JP, Peddibhotla S, Bu W, Zhao J, Haricharan S, Du YC, Podsypanina K, Rosen JM, Donehower LA, Li Y. Defining the ATM-mediated barrier to tumorigenesis in somatic mammary cells following ErbB2 activation. Proceedings of the National Academy of Sciences of the United States of America. 2010; 107:3728–3733. [PubMed: 20133707]

Sambade MJ, Peters EC, Thomas NE, Kaufmann WK, Kimple RJ, Shields JM. Melanoma cells show a heterogeneous range of sensitivity to ionizing radiation and are radiosensitized by inhibition of B-RAF with PLX-4032. Radiotherapy and oncology : journal of the European Society for Therapeutic Radiology and Oncology. 2011; 98:394–399. [PubMed: 21295875]

Sancar A, Lindsey-Boltz LA, Unsal-Kacmaz K, Linn S. Molecular mechanisms of mammalian DNA repair and the DNA damage checkpoints. Annual review of biochemistry. 2004; 73:39–85.

Schmitt MW, Kennedy SR, Salk JJ, Fox EJ, Hiatt JB, Loeb LA. Detection of ultra-rare mutations by next-generation sequencing. Proceedings of the National Academy of Sciences of the United States of America. 2012; 109:14508–14513. [PubMed: 22853953]

Smith J, Larue L, Gillespie DA. Chk1 is essential for the development of murine epidermal melanocytes. Pigment cell & melanoma research. 2013; 26:580–585. [PubMed: 23557358]

Soria G, Speroni J, Podhajcer OL, Prives C, Gottifredi V. p21 differentially regulates DNA replication and DNA-repair-associated processes after UV irradiation. Journal of cell science. 2008; 121:3271–3282. [PubMed: 18782865]

Sproul CD, Mitchell DL, Rao S, Ibrahim JG, Kaufmann WK, Cordeiro-Stone M. Cyclobutane Pyrimidine Dimer Density as a Predictive Biomarker of the Biological Effects of Ultraviolet Radiation in Normal Human Fibroblast. Photochemistry and photobiology. 2014; 90:145–154.

Sproul CD, Rao S, Ibrahim JG, Kaufmann WK, Cordeiro-Stone M. Is activation of the intra-S checkpoint in human fibroblasts an important factor in protection against UV-induced mutagenesis? Cell cycle. 2013; 12:3555–3563. [PubMed: 24091629]

Stankovic T, Stewart GS, Byrd P, Fegan C, Moss PA, Taylor AM. ATM mutations in sporadic lymphoid tumours. Leukemia & lymphoma. 2002; 43:1563–1571. [PubMed: 12400598]

Suram A, Kaplunov J, Patel PL, Ruan H, Cerutti A, Boccardi V, Fumagalli M, Di Micco R, Mirani N, Gurung RL, et al. Oncogene-induced telomere dysfunction enforces cellular senescence in human cancer precursor lesions. The EMBO journal. 2012; 31:2839–2851. [PubMed: 22569128]

Swope V, Alexander C, Starner R, Schwemberger S, Babcock G, Abdel-Malek ZA. Significance of the melanocortin 1 receptor in the DNA damage response of human melanocytes to ultraviolet radiation. Pigment cell & melanoma research. 2014; 27:601–610. [PubMed: 24730569]

Thomas NE, Edmiston SN, Alexander A, Millikan RC, Groben PA, Hao H, Tolbert D, Berwick M, Busam K, Begg CB, et al. Number of nevi and early-life ambient UV exposure are associated with BRAF-mutant melanoma. Cancer epidemiology, biomarkers & prevention : a publication of the American Association for Cancer Research, cosponsored by the American Society of Preventive Oncology. 2007; 16:991–997.

Unsal-Kacmaz K, Chastain PD, Qu PP, Minoo P, Cordeiro-Stone M, Sancar A, Kaufmann WK. The human Tim/Tipin complex coordinates an Intra-S checkpoint response to UV that slows replication fork displacement. Molecular and cellular biology. 2007; 27:3131–3142. [PubMed: 17296725]

Unsal-Kacmaz K, Mullen TE, Kaufmann WK, Sancar A. Coupling of human circadian and cell cycles by the timeless protein. Molecular and cellular biology. 2005; 25:3109–3116. [PubMed: 15798197]

Vredeveld LC, Possik PA, Smit MA, Meissl K, Michaloglou C, Horlings HM, Ajouaou A, Kortman PC, Dankort D, Mcmahon M, et al. Abrogation of BRAFV600E–induced senescence by PI3K pathway activation contributes to melanomagenesis. Genes & development. 2012; 26:1055–1069. [PubMed: 22549727]

Wang X, Guan J, Hu B, Weiss RS, Iliakis G, Wang Y. Involvement of Hus1 in the chain elongation step of DNA replication after exposure to camptothecin or ionizing radiation. Nucleic acids research. 2004; 32:767–775. [PubMed: 14762204]

Watts KP, Fairchild RG, Slatkin DN, Greenberg D, Packer S, Atkins HL, Hannon SJ. Melanin content of hamster tissues, human tissues, and various melanomas. Cancer research. 1981; 41:467–472. [PubMed: 7448793]

Yamada A, Masutani C, Iwai S, Hanaoka F. Complementation of defective translesion synthesis and UV light sensitivity in xeroderma pigmentosum variant cells by human and mouse DNA polymerase eta. Nucleic acids research. 2000; 28:2473–2480. [PubMed: 10871396]

Yu H, Mcdaid R, Lee J, Possik P, Li L, Kumar SM, Elder DE, Van Belle P, Gimotty P, Guerra M, et al. The role of BRAF mutation and p53 inactivation during transformation of a subpopulation of primary human melanocytes. The American journal of pathology. 2009; 174:2367–2377. [PubMed: 19389934]

Zou L, Elledge SJ. Sensing DNA damage through ATRIP recognition of RPA-ssDNA complexes. Science. 2003; 300:1542–1548. [PubMed: 12791985]

Significance

Transformation of melanocytes to melanomas frequently involves mutational activation of *BRAF* or and *NRAS* oncogenes. As these oncogenes cause melanocytes to undergo senescence, melanoma development requires bypass of this barrier. Oncogenes are known to induce replication stress that may trigger intra-S checkpoint responses to enforce senescence. It was, therefore, important to determine whether the intra-S checkpoint responses to UVC-induced replication stress were attenuated or inactivated in melanoma cell lines. Melanoma cell lines were found to retain intra-S checkpoint responses to UVC-induced DNA damage. This might be because some of the proteins that are required for checkpoint function (e.g., ATR and Chk1) are also essential for cell viability.

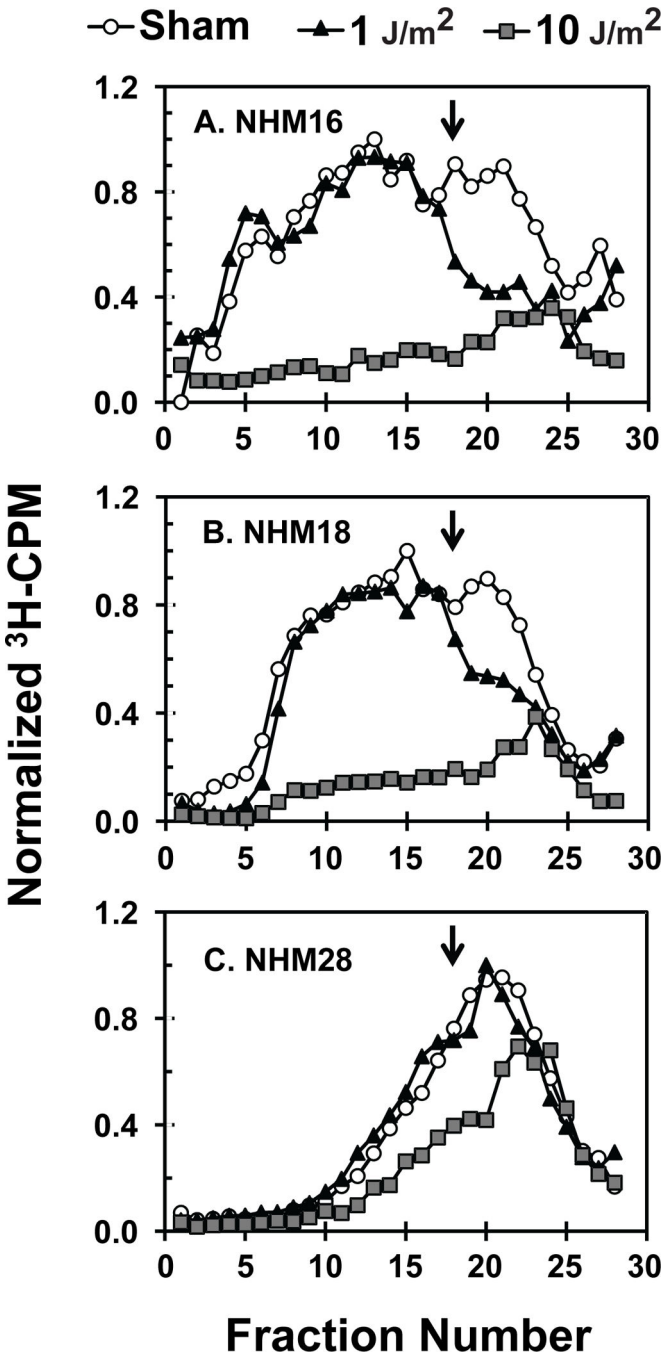

Figure 1.

Velocity sedimentation analysis discloses both active and passive responses to UVC-induced DNA damage. Normal human melanocytes with nuclear DNA homogeneously labeled with [^{14}C]thymidine were exposed to increasing fluences of UVC, incubated for 30 min, pulse-labeled for 15 min with [^{3}H]thymidine, and lysed on top of 5–20% alkaline sucrose gradients. After sedimentation and fractionation, acid-insoluble radioactivity was quantified. The graphs illustrate the size distributions of radiolabeled single-stranded DNA in NHM16 (A), NHM18 (B) and NHM28 (C) melanocyte cultures exposed to zero (sham;

white-filled circles), 1 J/m^2 (black-filled triangles), or 10 J/m^2 (gray-filled squares) of 254 nm UVC radiation (see Supplementary Figure S2 for results with other UVC fluences). Normalized ^{3}H-CPM represents the radioactivity incorporated into nascent DNA of various sizes during the 15-min pulse with [^{3}H]thymidine, relative to the total number of cells added to each gradient (as measured by the total ^{14}C-CPM) and to the highest value in the experimental group. This normalization also illustrates the extent of DNA synthesis inhibition by each of the UVC fluences. The profile observed in the cultures exposed to 1 J/m^2 UVC, compared to the sham control, revealed (as illustrated in A and B) a selective inhibition in molecules with sizes less than 60 kb (marked by the arrow), consistent with the intra-S checkpoint response of inhibition of replicon initiation (see also Fig. 2A). A larger and cytotoxic fluence of UVC (10 J/m^2) produced a strong inhibition of DNA synthesis in active replicons (gradient fractions 5–17), due to blockage of DNA polymerases at template lesions (passive inhibition) and active checkpoint signaling, with a concomitant appearance of a peak of abnormally small DNA (in fractions 21–25) that heralds the presence of daughter-strand gaps. The smaller size of nascent DNA seen in NHM28 may be the result of enhanced fluorescent-light-induced fragmentation of DNA during cell lysis due to high melanin content of the cells.

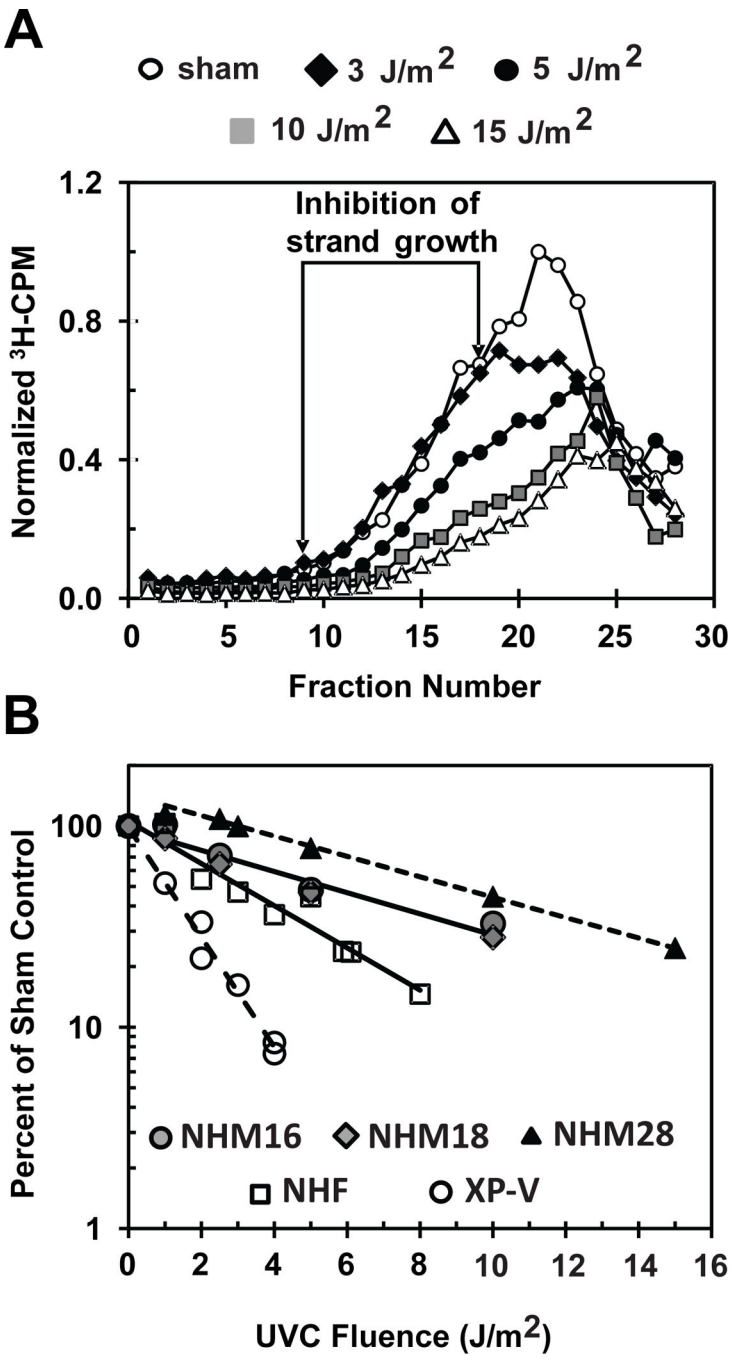

Figure 2.

UVC-induced inhibition of DNA strand growth in diploid human cells. (A) Results of a second velocity sedimentation experiment with NHM28 using higher fluences of UVC (Sham, white-filled circles; 3.0 J/m^2, black-filled diamonds; 5 J/m^2, black-filled circles; 10 J/m^2, gray-filled squares; 15 J/m^2, white-filled triangles). Note the evidence for selective inhibition of low molecular weight nascent DNA (fractions 20–24) upon irradiation with 3 J/m^2 UVC (inhibition of replicon initiation). As the incident UVC fluence was increased, radiolabeled precursor incorporation in large molecular weight DNA intermediates (range

between the two arrows) decreased. The equivalent ranges of fractions from all gradients with the same cell type were used to quantify the UVC-dependent inhibition of DNA strand growth. (B) The decrease in radiolabel incorporation in high molecular weight intermediates of DNA replication, relative to the non-irradiated (sham) controls (average of duplicate experiments) was plotted against UVC fluence. Results with normal melanocytes (filled symbols: gray circle, NHM16; gray diamond, NHM18; and black triangles, NHM28) were compared to those previously published for two NHF lines (squares) and an XP-V cell line (circles) (King et al., 2005). The slopes determined for the NHF and XP-V lines were equivalent to slopes quantified in different NHF and XP-V strains in an earlier study (Kaufmann and Cleaver, 1981).

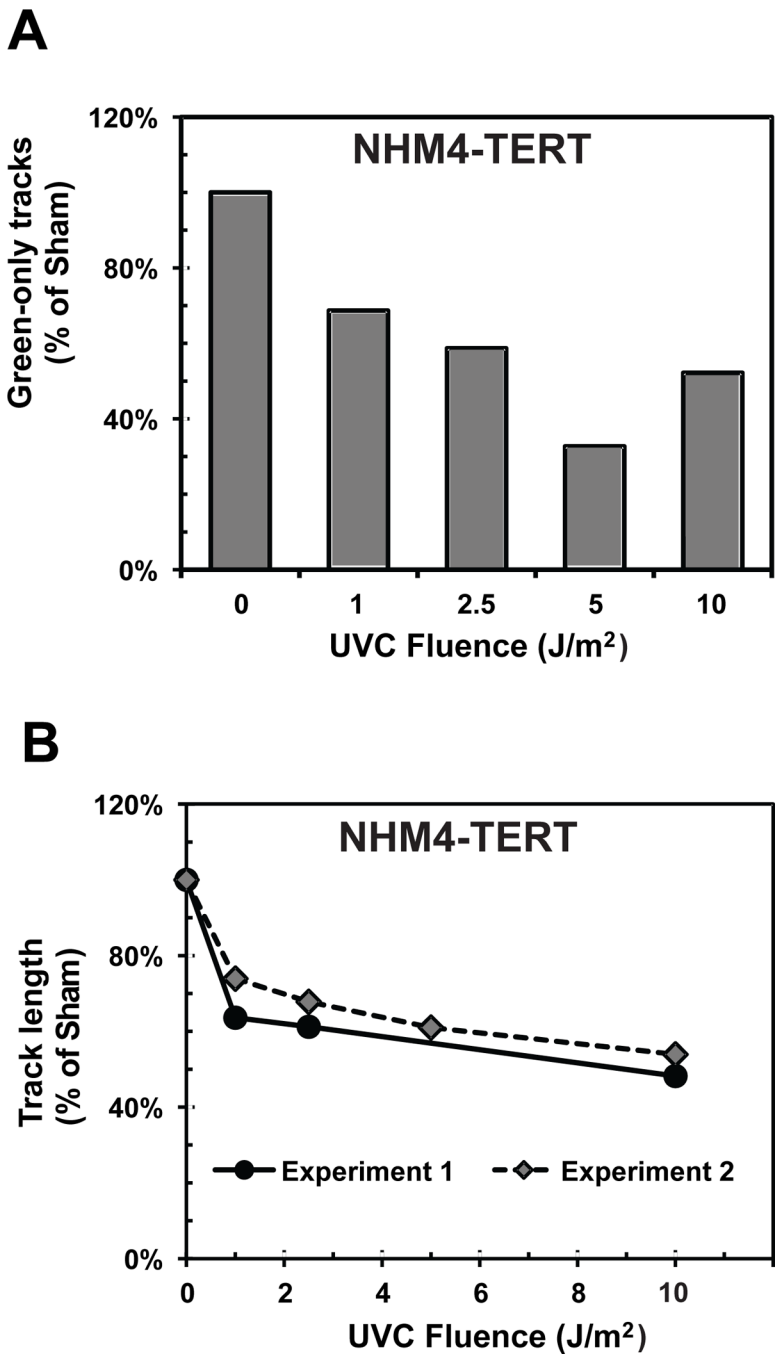

Figure 3.

UVC-induced inhibition of replicon initiation and DNA chain elongation in an immortalized normal human melanocyte line. NHM4-hTERT in log phase growth were pulse labeled with IdU for 15 min, exposed to the indicated fluences of UVC, then incubated in CldU-containing medium for 30 min. Individual DNA fibers were spread and immuno-stained as previously described (Chastain et al., 2006). Replication tracts containing IdU (pre-label) were stained red and those containing CldU (post-label) were stained green. (A) Frequency of green-only tracks (replicons initiated after UVC exposure) in irradiated samples, relative

to the sham control. The reduction in this class of labeled fibers indicates the degree of inhibition of replicon initiation by UVC. Results represent the average of two independent experiments in which 345 to 1036 individual fibers were counted in each sample. (B) UVC-dependent inhibition of DNA chain elongation. Labeled fibers with a green portion (CldU label) attached to a red portion (IdU) indicated replication units that were active before UVC exposure and continued to synthesize DNA after irradiation (green portion). The average length of the green portion of red-green tracks was measured in 39–71 individual fibers in each sample of two independent experiments. The inhibition curves show two distinct components: the sharp decrease in track length after 1 J/m^2 UVC appears to reflect the intra-S checkpoint-dependent, active slowing of DNA chain elongation; as the UVC fluence was increased further, the subsequent reduction in relative track length seems to include the contribution of passive inhibition of chain elongation at DNA template lesions.

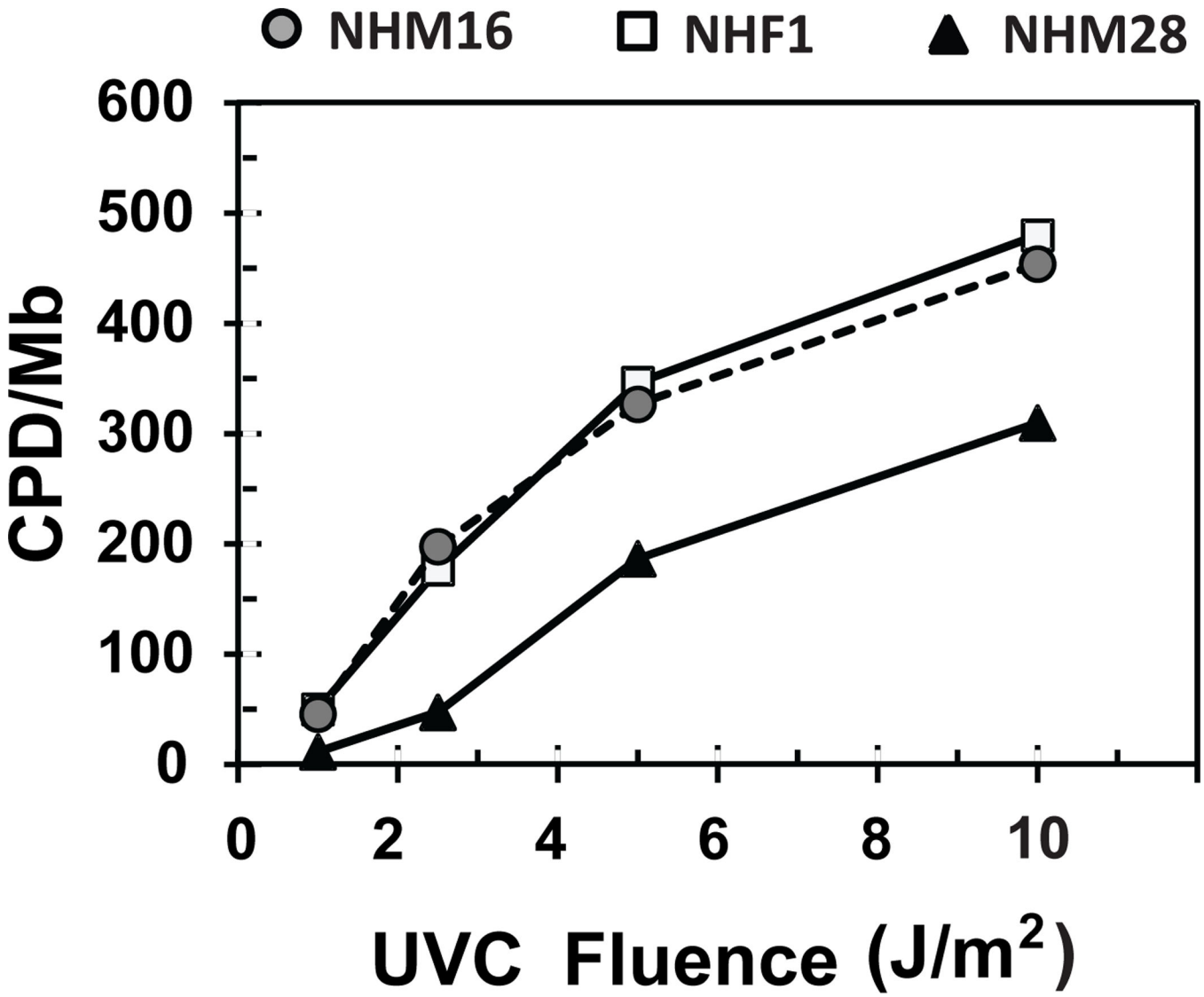

Figure 4.

CPD dosimetry in melanocytes and fibroblasts. Monolayer cultures of NHF1 fibroblasts (white squares), NHM16 melanocytes (gray-filled circles) and NHM28 melanocytes (black-filled triangles) were irradiated with the indicated fluences of UVC, and harvested immediately afterwards for DNA purification and CPD quantification by immunoblotting (Sproul et al., 2014). Illustrated results represent the averages of two independent experiments for each of the identified cultured cells. Quantification of melanin content (Watts et al., 1981) yielded the following values: NHM16, 15 μg/10^6 cells; NHM28, 39 μg/10^6 cells.

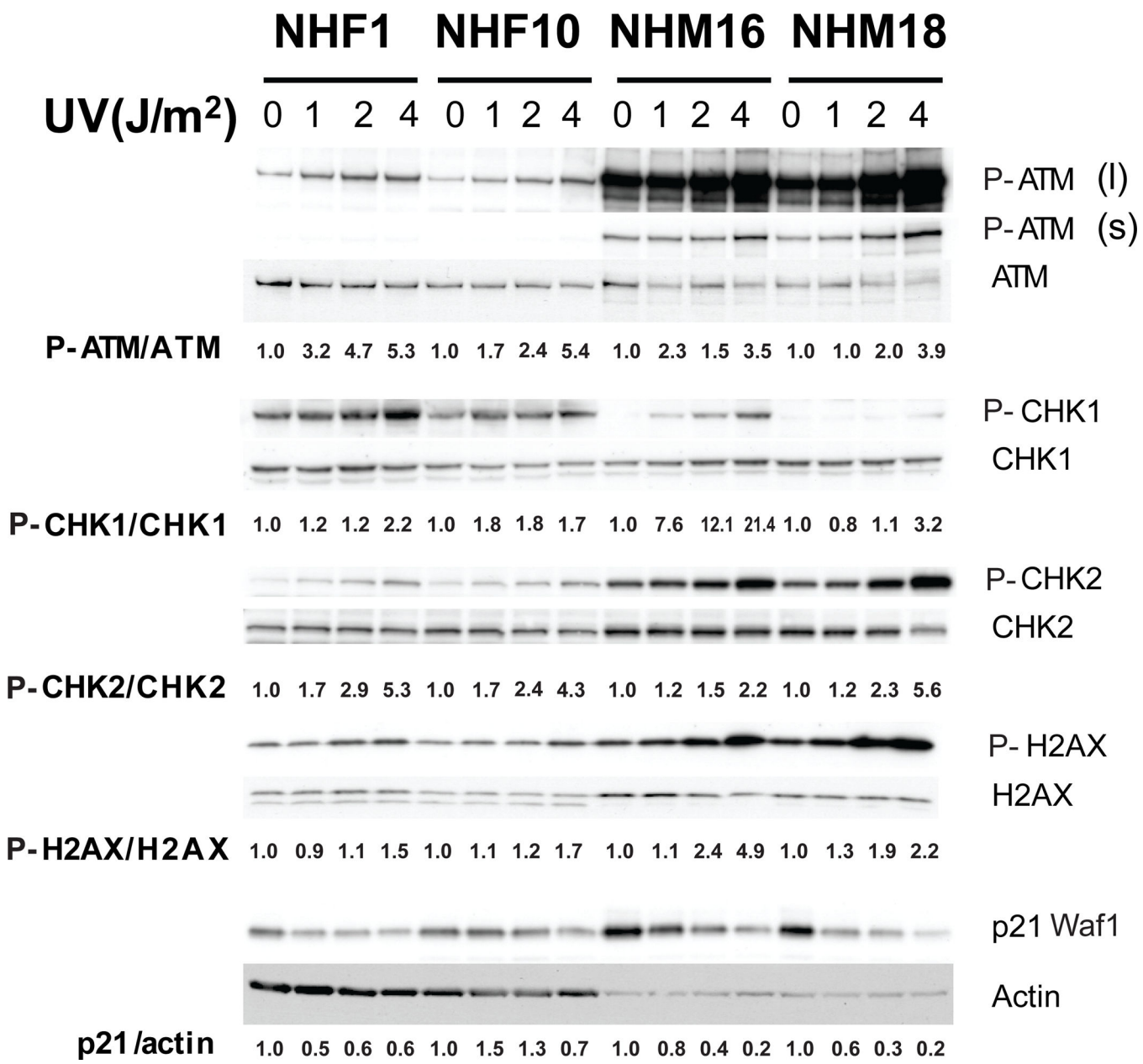

Figure 5.

DNA damage response markers in normal fibroblasts and melanocytes. Whole cell extracts were prepared from NHM16 and NHM18 melanocytes 45 min after exposure to the indicated fluences of UVC. Parallel experiments were also done with NHF1-hTERT and NHF10-hTERT fibroblasts. After gel electrophoresis and transfer to nitrocellulose, the membranes were probed with the indicated antibodies (see METHODS for details). Phospho-proteins were probed before the same membranes were stripped and then re-probed with the antibodies recognizing the modified and unmodified forms of the same proteins. Short (s) and long (l) exposures were used to detect the P-ATM signals. Image J was used to quantify the immunoblot signals from unsaturated X-ray films and the ratios of the

phosphorylated form over the total for each protein were determined and expressed relative to the same parameter determined in the sham-treated control (set as 1.0).

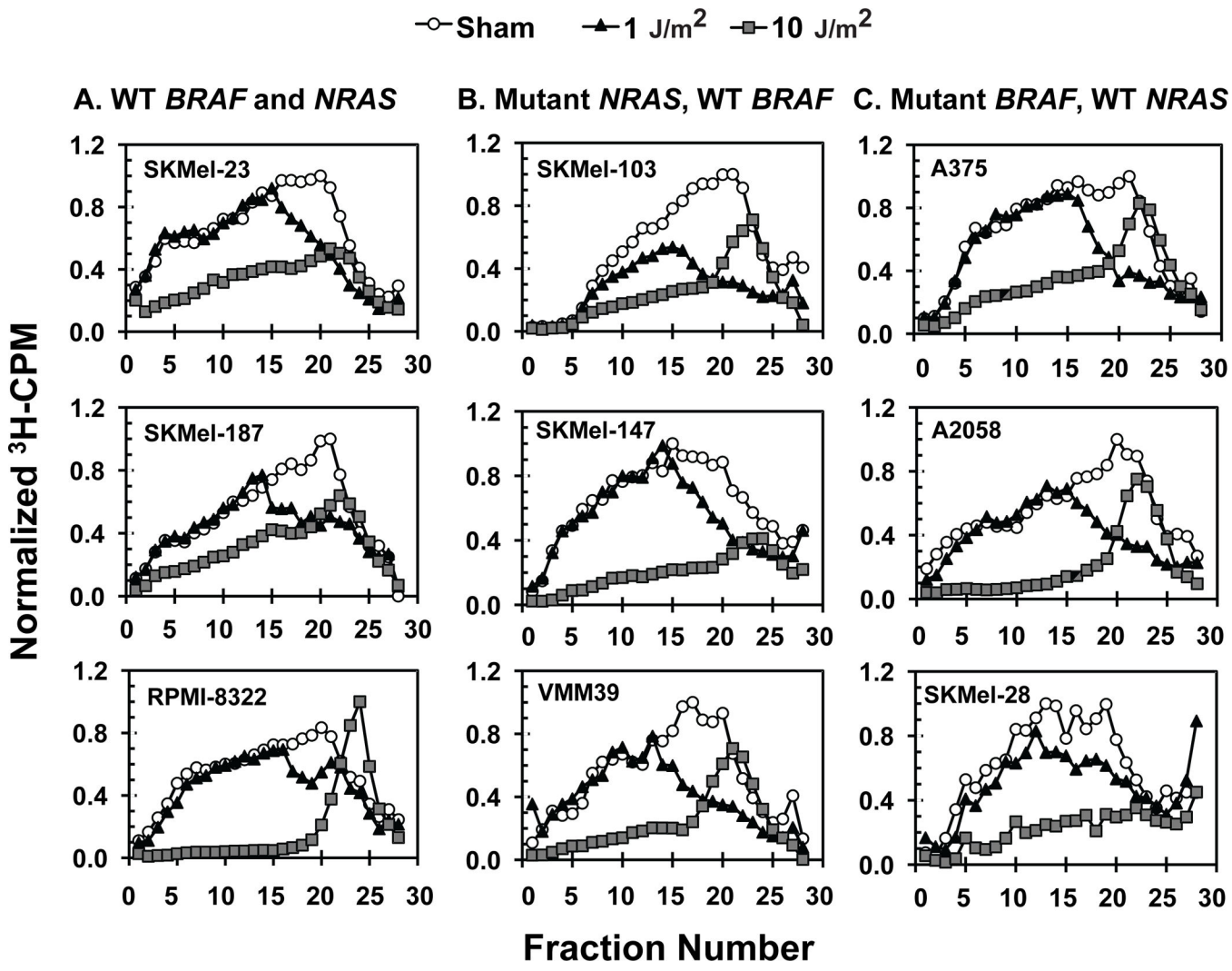

Figure 6.

Velocity sedimentation analysis of DNA replication in melanoma cell lines. Three cell lines were chosen (without previous knowledge of their response to UVC at the level of DNA replication) from each of three melanoma groups, based on the mutation status at the *BRAF* and *NRAS* loci: (A) Expressing wild type B-Raf and N-Ras; (B) Expressing a mutant N-Ras; (C) Expressing a mutant B-Raf. The experimental procedure was the same as described in the legend to Figure 1. The illustrated profiles are those for the sham-treated sample (white circles), and for the cells irradiated with 1 J m^2 UVC (black-filled triangles) or 10 J/m^2 UVC (gray-filled squares). Supplementary Figure S4 includes the results with 2.5 and 5 J/m^2 UVC. Note that after 1 J/m^2 UVC, all cell lines inhibited incorporation into nascent DNA of low molecular weight (inhibition of replicon initiation), albeit to different degrees. The pattern seen with RPMI 8322 was distinct from the other cell lines in that a minor peak of abnormally small DNA was already apparent at 1 J/m^2 and when the UVC fluence was increased to 10 J/m^2 the peak of abnormally small DNA rose above the control profile. SKMel-23 was first scored as wild-type for *BRAF* and *NRAS*. After subsequent studies

revealed behavior similar to B-Raf-mutant lines (Sambade et al., 2011), reanalysis identified a rare *BRAF* mutation (G466A).

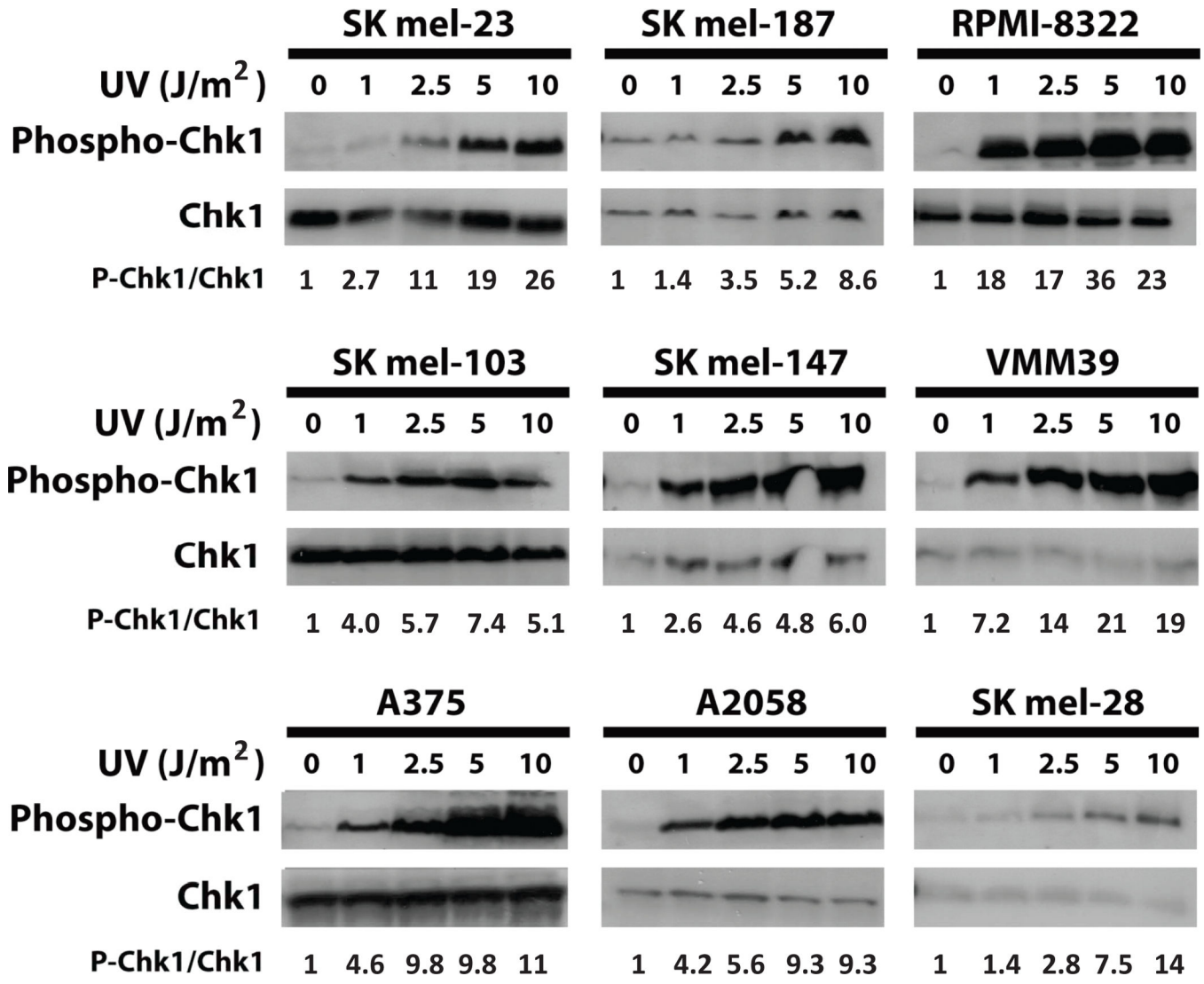

Figure 7.

UVC induction of Chk1 phosphorylation in melanoma cell lines. The experimental details were as described in the legend to Figure 5.

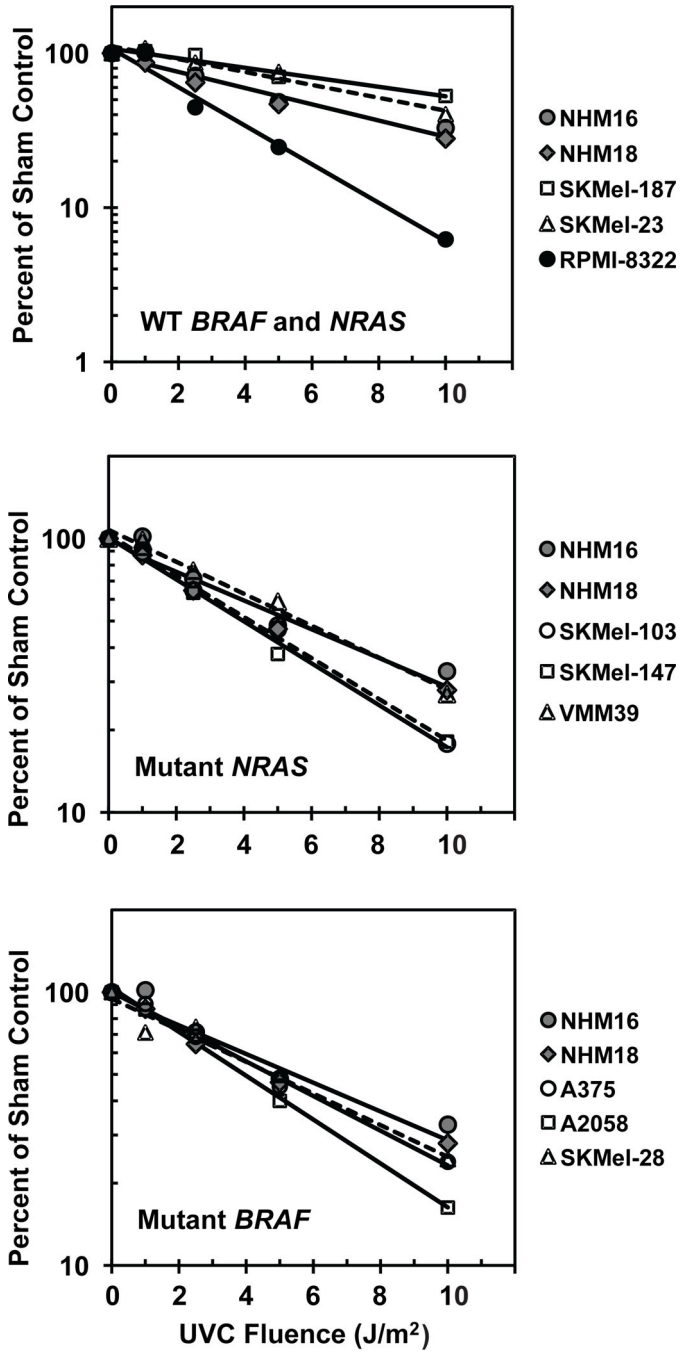

Figure 8.

Inhibition of DNA strand growth by UVC in melanoma cell lines. The average results of inhibition of incorporation of radiolabeled [^{3}H]thymidine in high molecular weight nascent DNA species (see Figure 2) from 2–3 independent experiments for each cell line were plotted against UVC fluences (no significant differences in CPD densities were expected among the different melanomas and NHM16 and NHM18 – see text). The slopes determined for each line are reported in Table 1. Only RPMI 8322 displayed results that were clearly distinct from the normal melanocytes and the other melanoma cell lines ($p<0.0001$).

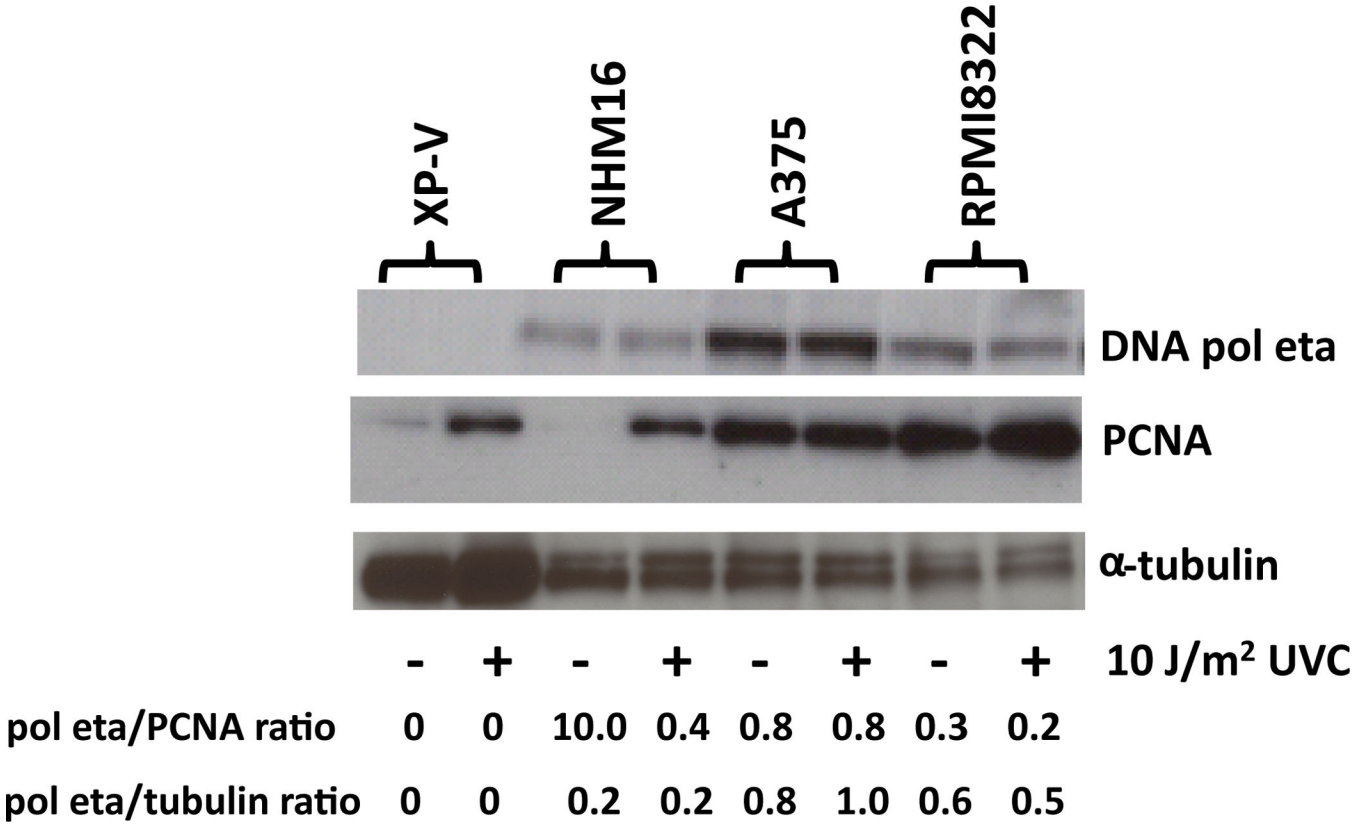

Figure 9.

Relative abundance of DNA polymerase eta. Chromatin was isolated from the indicated cultured cells 45 min after sham treatment (−) or irradiation with 10 J/m^2 UVC (+). Twenty five micrograms of chromatin protein from each sample were loaded onto polyacrylamide gels. Following gel electrophoresis and transfer to a nitrocellulose membrane, the chromatin-associated proteins were probed with antibodies against DNA pol eta, PCNA and α-tubulin. XP-V fibroblasts were included as a negative control for DNA pol eta expression. Pixel intensity values in unsaturated X-ray films were quantified for each protein. The levels of DNA pol eta were expressed relative to PCNA and α-tubulin.

Table 1

Slopes of Inhibition of DNA Strand Growth

Melanocytes	Slope	Intercept	Correlation Coefficient
NHM16	−0.052	2.007	−0.969
NHM18	−0.053	1.962	−0.992
NHM16&18 Combined	−0.053	1.984	−0.972
NHM28	−0.051	2.153	−1.000
Fibroblasts			
NHF	−0.105	2.023	−0.967
XPV	−0.272	1.992	−0.990

Melanomas	Slope	Intercept	Correlation Coefficient	*P* value[1]
WT *BRAF* and *NRAS*				
SKMel-187	−0.031	2.029	−0.974	0.0004
RPMI-8322	−0.125	2.029	−0.993	<0.0001
Mutant *NRAS*, WT *BRAF*				
VMM39	−0.058	2.032	−0.994	0.5517
SKMel-103	−0.075	2.014	−0.998	<0.0001
SKMel-147	−0.077	2.004	−0.995	<0.0001
Mutant *BRAF*, WT *NRAS*				
SKMel-28	−0.058	1.976	−0.984	0.0335
A375	−0.063	2.000	−0.997	0.0115
A2058	−0.080	2.015	−0.999	<0.0001
SKMel-23[2]	−0.042	2.045	−0.978	0.0119

[1] Statistical difference between the slopes determined for each melanoma cell line, compared to that defined by the combined NHM16 and NHM18 data points.

The RPMI-8322 slope was also significantly different from those determined for all the other melanoma cell lines ($p<0.0001$). Within the mutant *NRAS* group, the slopes for SKMel-103 and SKMel-147 were the same, but statistically different from that of VMM39 ($p=0.0002$ and $p<0.0001$, respectively). In the mutant *BRAF* group, A2058 is the cell line with the most statistically different slope ($p=0.0028$ by comparison with A375, and $p=0.0009$ by comparison with SKMel-28.

[2] SKMel-23, first scored as wild-type for *BRAF* and *NRAS*, was later found to carry a rare *BRAF* mutation G466A (Sambade et al., 2011).